Three-Dimensional Quantitative Structure−Activity Relationships of Mazindol Analogues at the Dopamine Transporter

Santosh S. Kulkarni,[†] Amy Hauck Newman,*[,†] and William J. Houlihan[‡]

Medicinal Chemistry Section, National Institute on Drug Abuse—Intramural Research Program, National Institutes of Health, 5500 Nathan Shock Drive, Baltimore, Maryland 21224, and Charles A. Dana Research Institute, Hall of Sciences, Room 331, Drew University, Madison, New Jersey 07940

Received May 11, 2001

A three-dimensional quantitative structure−activity relationship (3D-QSAR) study was performed on a series of mazindol analogues using the comparative molecular field analysis (CoMFA) method with their corresponding binding affinities for the displacement of [^{3}H]WIN 35 428 from rat caudate putamen tissue. The cross-validated CoMFA models were derived from a training set of 50 compounds, and the predictive ability of the resulting CoMFA models was evaluated against a test set of 21 compounds. A set of alignment rules was derived to superimpose these compounds onto a template structure, mazindol (**1**). These CoMFA models yielded significant cross-validated r^2_{cv} values. Inclusion of additional descriptors did not improve the significance of the CoMFA models; thus, steric and electrostatic fields are the relevant descriptors for these compounds. The best QSAR model was selected on the basis of the predictive ability of the activity on the external test set of compounds. The analysis of coefficient contour maps provided further insight into the binding interactions of mazindol analogues with the DAT. The aromatic rings C and D are involved in hydrophobic interactions in which ring D may bind in a large hydrophobic groove. The relative orientation of these two rings is also important for high binding affinity to the DAT.

Introduction

Cocaine binds with moderate affinity to all three of the monoamine transporters and subsequently inhibits the reuptake of the neurotransmitters dopamine, serotonin, and norepinephrine into their respective neurons. Studies investigating molecular targets for the pharmacological and behavioral effects of cocaine have led to the identification of the dopamine transporter (DAT) as a primary molecular site of action.[1−3] A review of the literature shows that the development of cocaine abuse therapies continues to focus primarily on drugs that selectively target the DAT.[4−8] Thus, thorough understanding of the structure and function of the DAT is essential for the development of drugs for cocaine abuse treatment. To date, the DAT has been cloned and expressed, but its 3D structure is unknown.[9−12] However, considerable research has been conducted to identify the cocaine recognition site using selective high-affinity ligands.[5]

Mazindol (5-(4-chlorophenyl)-2,3-dihydro-5*H*-imidazo [2,1-*a*] isoindol-5-ol) **1** is a compound that inhibits the uptake of dopamine, serotonin, and norephinephrine at their respective monoamine transporters.[13,14] It inhibits the uptake of dopamine in rat striatal synaptosomes and cells expressing the human and rat DAT and also inhibits binding of [^{3}H]cocaine and [^{3}H]WIN 35 428 in the nanomolar range.[15] Although mazindol and cocaine have been reported to occupy a similar binding site at the DAT,[16−18] a lack of correlation of their effects on [^{3}H]-WIN 35 428 binding in the rat caudate putamen and stimulant effects in the mouse locomotor assay suggests that they may bind in a fundamentally different manner.[19] Clinical studies with mazindol have shown some encouraging results, necessitating further evaluation of mazindol analogues as potential cocaine abuse therapeutics.[20−23]

A series of mazindol analogues have been synthesized and tested for binding at the DAT.[24−27] These SAR studies were focused on how modification of the pendant aryl group and substitution with different functional groups on these aromatic rings affected DAT binding affinities.[24−26] Also, the effect of increasing the size of the heterocyclic and fused benzene or cyclohexane rings at various positions was investigated. Some open-chain analogues of mazindol have been reported.[27] These SAR studies have provided a dataset of diverse compounds with a wide spectrum of affinities for DAT.

To rationalize the observed variance in biological activity of these analogues and to develop a model from which additional DAT ligands could be designed, we derived a three-dimensional quantitative structure−activity relationship (3D-QSAR) by comparative molecular field analysis (CoMFA).[28] A preliminary analysis of mazindol analogues showed the importance of different structural features for activity on the DAT. The CoMFA models were derived and then used to further characterize the optimal binding requirements for mazindol analogues at the DAT.

Methods

Biological Activity. A set of 71 mazindol analogues was selected for the present CoMFA study. Because there is a variation in biological activity measured under different

* To whom correspondence should be addressed. Phone: 410-550-1455. Fax: 410-550-1648. Email: anewman@intra.nida.nih.gov.
[†] National Institutes of Health.
[‡] Drew University.

10.1021/jm0102093 CCC: $22.00
Published on Web 01/22/2002

Table 1. Structures and Activities of Mazindol Analogues

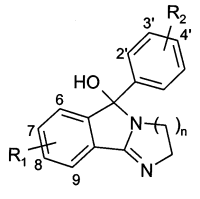

				observed activity		
compd	R_1	R_2	*n*	IC_{50}[a]	$p(IC_{50})$[b]	predicted activity[c]
1	H	4′-Cl	1	8.1 ± 1.2	2.0915	1.9198
2	H	4′-Cl	2	1.0 ± 0.2	3.0000	2.5465
3	H	4′-Cl	3	1.5 ± 0.1	2.8239	2.7564
4	H	H	1	66 ± 8.9	1.1805	0.7126
5	H	H	3	5.9 ± 0.1	2.2291	2.0528
6	H	2′-Cl	1	290 ± 6	0.5317	0.7528
7	H	2′-Br	1	1300 ± 180	−0.1271	0.5038
8	H	2′-F	2	23 ± 1.7	1.6345	1.0829
9	H	3′-Cl	1	4.3 ± 0.4	2.3665	1.5097
10	H	3′-CF_3	1	230 ±17	0.6383	0.4080
11	H	3′-F	2	2.0 ± 0.02	2.6990	2.1215
12	H	4′-F	1	13 ± 1.8	1.8761	1.8202
13	H	4′-F	2	3.2 ± 1.7	2.4949	2.2923
14	H	4′-I	1	17 ± 0.9	1.7645	1.6193
15	H	4′-$CH_2N(CH_3)_2$	1	2800 ± 200	−0.4425	−0.2258
16	H	4′-OH	2	3.4 ± 0.4	2.4685	2.3300
17	H	4′-OCH_3	2	2.5 ± 0.1	2.6021	2.3911
18	H	4′-$OCH_2CH{=}CH_2$	2	72 ± 8.2	1.1457	1.2916
19	H	4′-$OCH_2C_6H_5$	2	100 ± 5.8	1.0008	0.6526
20	H	3′,4′-$(Cl)_2$	1	2.5 ± 0.5	2.6021	2.1470
21	H	3′,4′-$(OCH_3)_2$	2	87 ± 13	1.0585	1.7217
22	6-Cl	H	1	57 ± 8.3	1.2426	1.0160
23	7-Cl	H	1	86 ± 14	1.0635	1.3281
24	7-Cl	4′-F	1	53 ± 8.7	1.2774	1.4851
25	7-F	4′-Cl	1	6.5 ± 1.2	2.1871	2.1493
T26[d]	H	H	2	5.8 ± 1.6	2.2366	1.9422
T27[d]	H	3′-Cl	2	1.0 ± 0.2	3.0000	2.1712
T28[d]	H	4′-Br	1	2.6 ± 1.5	2.5850	1.8313
T29[d]	H	4′-$CH_2OC_6H_5$	1	720 ± 37	0.1415	−0.5601
T30[d]	H	4′-CH_3	1	93 ± 8.7	1.0301	1.2852
T31[d]	H	4′-CF_3	1	290 ± 31	0.5376	0.9399
T32[d]	H	4′-$COOCH_3$	1	3300 ± 45	−0.5198	1.1246
T33[d]	H	4′-$CH_2NCH_2(CH_2)_3CH_2$	2	1200 ± 180	−0.0682	0.5010
T34[d]	H	2′,4′-$(Cl)_2$	1	77 ± 1.1	1.1163	1.1472
T35[d]	H	3′,4′-$(OCH_3)_2$	1	6900 ± 700	−0.8382	−1.0895
T36[d]	H	3′,4′-$(Cl)_2$	3	1.7 ± 0.1	2.7696	2.8705
T37[d]	7,8-$(Cl)_2$	4′-Cl	1	14 ± 1.5	1.8665	2.0146

[a] Biological activity expressed in nM. Data from refs 24−27. [b] Expressed as the logarithm of $1/IC_{50}$ (μM) value. [c] Predicted from the CoMFA model from alignment I. [d] Molecules belonging to the test set.

conditions, it is essential to select compounds tested under identical experimental conditions. We selected those compounds, which were tested in rat caudate putamen, to inhibit the binding of [^{3}H]WIN 35 428 under identical assay conditions.[24−27] The logarithm of the $1/IC_{50}$ value was used as a dependent variable in the present study. The structures of inhibitors and their activities are presented in Tables 1−5. The predictive power of the CoMFA models was evaluated by setting aside 21 compounds with uniform distribution of biological activity as a test set. The mean (standard deviation) of the biological activity of the training and test sets was 0.84 (1.28) and 0.85 (1.31), respectively.

Molecular Modeling. All computational studies were performed using the molecular modeling program SYBYL 6.6, running on a Silicon Graphics Octane workstation. The structural manipulations were performed using the standard TRIPOS force field. Partial atomic charges (Mulliken) of the molecules were calculated using the AM1 model Hamiltonian within MOPAC 6.0.[29]

All the analogues of mazindol were constructed from the standard fragment library in SYBYL. Structures were minimized using a conjugate gradient minimization algorithm until a gradient convergence of 0.001 kcal/(mol·Å) was reached. The conformational search on the cyclic analogues was performed by rotating the bond connecting the rings B and D. For open-chain compounds all the rotatable bonds were searched by rotating from 0° to 359° by 15° increments. Conformational energies were computed with an electrostatic term, and the

Table 2. Structures and Activities of Mazindol Analogues

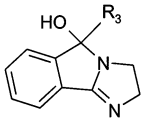

		observed activity		predicted
compd	R_3	IC_{50}[a]	$p(IC_{50})$[b]	activity[c]
38	2-pyridyl	3700 ± 410	−0.5682	−0.7146
39	3-pyridyl	640 ± 52	0.1952	1.0544
40	2-furyl	19000 ± 3700	−1.2856	−1.2256
41	methyl	67000 ± 2100	−1.8243	−1.2577
42	*tert*-butyl	9500 ± 6800	−0.9777	−1.2506
43	1-methylcyclohex-1-yl	3500 ± 2700	−0.5441	−0.6323
44	1-adamantyl	4900 ± 200	−0.6857	−0.9986
T45[d]	4-pyridyl	63 ± 5.6	1.2041	1.3842
T46[d]	cinnamyl	9300 ± 440	−0.9685	−0.8260
T47[d]	2-naphthyl	23 ± 3.3	1.6334	1.8847

[a] Biological activity expressed in nM. Data from refs 24−27. [b] Expressed as the logarithm of $1/IC_{50}$ (μM) value. [c] Predicted from the CoMFA model from alignment I. [d] Molecules belonging to the test set.

Table 3. Structures and Activities of Mazindol Analogues

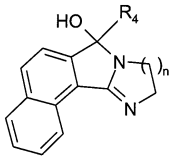

			observed activity[a]		
compd	R_4	*n*	IC_{50}[a]	$p(IC_{50})$[b]	predicted activity[c]
48	(4′-Cl)C_6H_4	1	16 ± 2.2	1.7967	1.5159
49	2-naphthyl	1	38 ± 6.5	1.4190	1.4897
50	(4′-Cl)C_6H_4	2	37 ± 1.5	1.4286	1.7513

[a] Biological activity expressed in nM. Data from refs 24−27. [b] Expressed as logarithm of $1/IC_{50}$ (μM) value. [c] Predicted from the CoMFA model from alignment I.

lowest energy conformer was selected and used for alignment in the CoMFA studies. The crystallographic data available on the 3-iodo analogue of mazindol were compared with the structure obtained from molecular manipulations in SYBYL.[30] The exact similarity (rmsd of non-hydrogen atoms is 0.112 Å) in the conformational data adds confidence in the modeling protocol used for generating the active conformations of the mazindol analogues.

Alignment Rules. The alignment, i.e., molecular conformation and orientation, is one of the sensitive inputs for a CoMFA study. The preliminary structure−activity analysis of mazindol analogues has shown the importance of hydrophobic ring structures for binding with the DAT. These important structural features of mazindol analogues can help to define the alignment rules for the present CoMFA study. The ultraviolet spectral studies have shown that mazindol occurs in the tricyclic (ol) form in neutral media, whereas in acidic media the protonated benzophenone (keto) form is preferred.[31] We considered the tricyclic (ol) form for all the cyclic compounds in order to model them under neutral physiological conditions. In these alignments, atom/centroids of the rings of the compounds were used for rms fitting onto the corresponding atom/centroids of the template structure, mazindol **1**. The atom/centroids of the rings used for alignments are defined in Table 6.

CoMFA Interaction Energies. The steric and electrostatic potential fields were calculated at each lattice intersection of a regularly spaced grid of 2.0 Å. The CoMFA region was defined automatically, and it extended past the van der Waals volume of all the molecules in *X*, *Y*, and *Z* directions. The steric and electrostatic fields were calculated using the default settings for the sp^3-hybridized carbon as a probe atom. The steric and electrostatic contributions were truncated to ±30 kcal/mol, and the electrostatic contributions were ignored at lattice intersections with maximal steric interactions.

Additional Descriptors. The standard CoMFA interaction fields were supplemented with additional descriptors to improve the QSAR results. The molar refractivity (CMR) and partition coefficients (ClogP) were calculated within SYBYL. Only one additional descriptor was added with CoMFA fields for each statistical analysis to avoid erroneous correlations.

Partial Least-Squares (PLS) Analysis. The partial least-squares algorithm was used in conjugation with the cross-validation (leave one out) option to obtain the optimum number of components, which were used to generate the final CoMFA model without cross-validation. The result from a cross-validation analysis was expressed as r^2_{cv}, which is defined as

$$r^2_{cv} = 1 - \frac{\text{PRESS}}{\sum (Y - Y_{mean})^2}$$

where $\text{PRESS} = \sum (Y - Y_{pred})^2$.

The optimum number of components was taken as the number required to increase r^2_{cv} by ~5% from the model with one fewer component rather than the default SYBYL estimate, which is based on highest r^2_{cv} value. Equal weights were assigned to steric and electrostatic descriptors using the CoMFA scaling option. All cross-validated PLS analyses were performed with a minimum σ (column filter) value of 2.0 kcal/mol, which minimized the influence of column noise and reduced the computation time. To obtain the statistical confidence limits of analysis, a bootstrapping analysis for 100 times was performed.

Prediction of Test Set Compounds. The CoMFA models derived from the training set of compounds were used to predict the activity of 21 compounds in a test set that were not included in the training set. The predictive r^2 (r^2_{pred}) will

Table 4. Structures and Activities of Open Chain Analogues of Mazindol

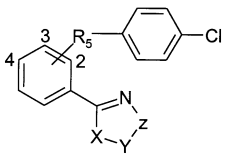

						observed activity		
compd	isomer	R_5	X	Y	Z	IC_{50}[a]	$p(IC_{50})$[b]	predicted activity[c]
51	2	C=O	NH	CH	CH	2800 ± 220	−0.4502	−0.7177
52	2	C=O	NCH_3	CH	CH	4300 ± 900	−0.6335	−0.9641
53	2	CH(OH)	NH	CH_2	CH_2	190 ± 36	0.7122	0.5245
54	2	CH(OH)	NH	CH_2	CH_2	2700 ± 160	−0.4302	−0.1262
55	2	C=O	O	CH_2	$C(CH_3)_2$	560 ± 150	0.2299	0.1925
56	2	S	NH	CH_2	CH_2	320 ± 36	0.5017	0.1961
57	2	S=O	NH	CH_2	CH_2	7300 ± 820	−0.8642	−0.8943
58	2	SO_2	NH	CH_2	CH_2	6500 ± 440	−0.8149	−0.6349
59	4	C=O	NH	CH_2	CH_2	3100 ± 150	−0.4853	−0.1147
60	4	C=O	O	CH_2	$C(CH_3)_2$	1900 ± 40	−0.2725	0.0509
61	4	CH(OH)	NH	CH_2	CH_2	1600 ± 82	−0.1942	−0.3828
62	4	CH(OH)	O	CH_2	$C(CH_3)_2$	3500 ± 170	−0.5441	−0.1356
T63[d]	2	O	NH	CH_2	CH_2	190 ± 2.6	0.7235	0.1339
T64[d]	2	CH_2	NH	CH_2	CH_2	4000 ± 530	−0.5978	0.4449
T65[d]	3	C=O	NH	CH_2	CH_2	2200 ± 150	−0.3483	0.2932
T66[d]	3	CH(OH)	O	CH_2	$C(CH_3)_2$	16000 ± 860	−1.2041	−0.0716

[a] Biological activity expressed in nM. Data from refs 24−27. [b] Expressed as logarithm of $1/IC_{50}$ (μM) value. [c] Predicted from the CoMFA model from alignment I. [d] Molecules belonging to the test set.

Table 5. Structures and Activities of Mazindol Analogues

comp. no.	Structure	observed activity		predicted activity[c]
		IC_{50}[a]	$p(IC_{50})$[b]	
67	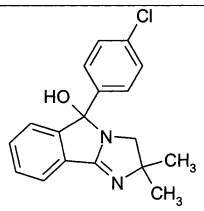	50 ± 5.5	1.2976	2.5116
68	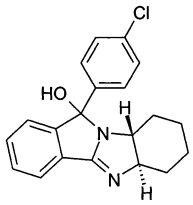	34 ± 1.40	1.4660	1.6774
69	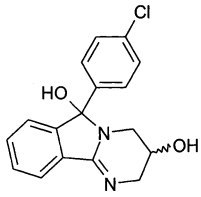	10 ± 1.1	2.0022	2.5836
T70[d]	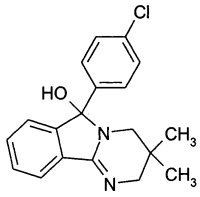	6.3 ± 4.5	2.2007	2.7475
T71[d]	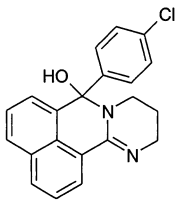	42 ± 3.0	1.3775	1.1925

[a] Biological activity expressed in nM. Data from refs 24−27. [b] Expressed as logarithm of $1/IC_{50}$ (μM) value. [c] Predicted from the CoMFA model from alignment I. [d] Molecules belonging to the test set.

Table 6. Atom/Centroids Used To Define Alignment Rules

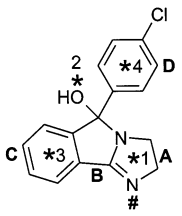

alignment rule	atom/centroids
I	*1, *2, *3, *4
II	*1, *3, *4
III	*1, *2, *3
IV	*1, *2, *4
V	*2, *3, *4
VI	#N, *2, *3, *4

be based on the molecules of the test set only and is defined as

$$r^2_{\text{pred}} = \frac{\text{SD} - \text{PRESS}}{\text{SD}}$$

Table 7. Summary of CoMFA Results

	alignment					
	I	II	III	IV	V	VI
r^2_{cv}	0.695	0.667	0.566	0.710	0.559	0.652
components	3	2	2	3	3	2
SEP	0.728	0.753	0.860	0.710	0.875	0.770
r^2_{ncv}	0.904	0.821	0.810	0.905	0.875	0.800
SEE	0.409	0.552	0.568	0.407	0.466	0.583
F value	144.227	107.502	100.452	145.854	107.304	94.001
P value	0.00	0.00	0.00	0.00	0.00	0.00
steric	52.9	49.8	49.4	46.7	42.6	49.4
electrostatic	47.1	50.2	50.6	53.3	57.4	50.6
r^2_{pred}	0.746	0.657	0.619	0.613	0.602	0.583
r^2_{bs}[a]	0.917	0.842	0.840	0.915	0.898	0.834
standard deviation[a]	0.025	0.039	0.038	0.026	0.029	0.035

[a] Results of bootstrapping analysis (100 samplings).

where SD is the sum of squared deviations between the biological activities of the test set and the mean activity of the training set molecules and PRESS is the sum of the squared deviation between the predicted and actual activity values for every molecule in the test set.

Results and Discussion

The CoMFA method was used to derive a 3D-QSAR model for mazindol analogues. The in vitro activity data on inhibition of [^{3}H]WIN 35 428 binding to the DAT were used as a dependent variable in this study. A diverse set of compounds were selected and are shown in Tables 1−5. The mazindol analogues contained two or three hydrophobic rings arranged in a rigid polycyclic structural framework in which one of the rings was heterocyclic. These analogues also contained a heteroatom, which may form a hydrogen bond or ionic type of interaction with the DAT. A series of open-chain compounds were also synthesized. These analogues (Table 4) contained all pharmacophoric elements of the cyclic analogues; however, their relative orientations were different. To align these molecules, it was essential to derive alternative alignment rules. Thus, these molecules were superimposed using the centroids of the hydrophobic rings rather than with the exact atom match. These alignments oriented the important pharmacophoric groups in the same three-dimensional space. The compounds were classified into training and test sets. The test set of compounds was utilized to assess the predictive ability of the CoMFA models derived from the training set. Twenty-one compounds (about 30% of the whole dataset) were selected as a test set, which represented the entire activity range, irrespective of their chemical compositions.

The results from the CoMFA studies are summarized in Table 7. The CoMFA-derived QSAR models showed considerable correlative and predictive properties. Alignment I showed a cross-validated $r^2 = 0.695$ with three components. A non-cross-validated $r^2 = 0.904$ with $F = 144.227$ was also observed with this model. The graph depicting the calculated vs observed activities of molecules used in building a QSAR model is shown in Figure 1. This graph depicts that less active compounds are more likely to be underpredicted than more active compounds. The observation of residuals across different classes of compounds does not show any trend, suggesting that the present CoMFA model represents the whole dataset of compounds. In this analysis almost equal contributions were observed from steric (52.9%) and

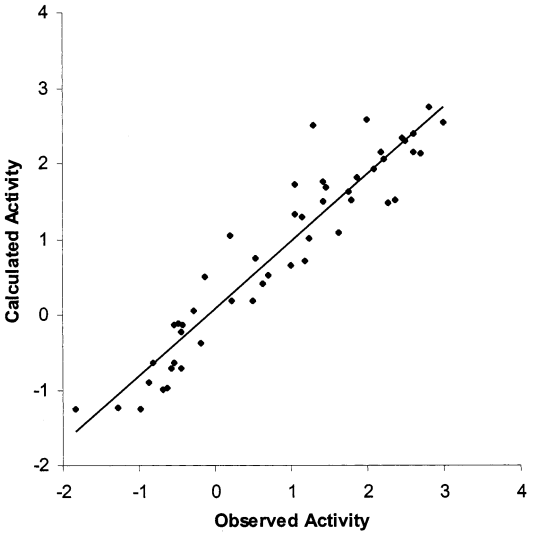

Figure 1. Calculated vs observed activity of molecules of the training set for the CoMFA analysis with alignment I.

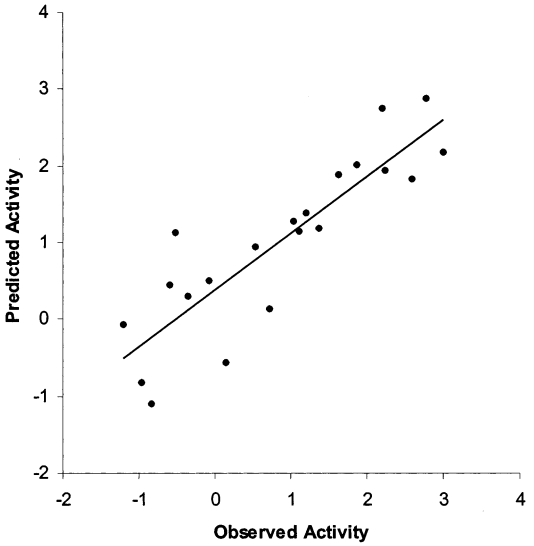

Figure 2. Predicted vs observed activity of the molecules of the test set with alignment I.

electrostatic (47.1%) fields. Previous CoMFA studies with dopamine uptake inhibitors have shown the importance of steric components over electrostatic interactions. For the phenyltropane compounds, the steric component was found to be the more relevant descriptor.[32,33] For the benztropine compounds, steric interactions supplemented with the hydrophobic parameter ClogP gave a highly correlative and predictive model.[34]

A predictive measure, r^2_{pred} of 0.746, was observed with the model (alignment I) for the mazindol analogues. Figure 2 shows the graph of predicted vs observed activity of test set molecules. Observation of the residuals showed that some of the compounds are not predicted optimally. The analysis of the residuals provided a measure of the predictability across different classes of the test set compounds. Compounds **T29** and **T46**, which contained larger substituents on ring D and were underpredicted, which might suggest that these compounds could have alternative binding orientations. A bootstrap analysis (100 sampling) was performed to obtain the confidence limits for this analysis. An r^2 bootstrap of 0.917 with a standard deviation of 0.025 suggested that a similar relationship exists for all of the compounds.

Table 8. CoMFA Results with Additional Descriptors

	descriptors				
	SE[a]	S	E	SE/ClogP	SE/CMR
r^2_{cv}	0.695	0.604	0.501	0.700	0.673
components	3	4	1	4	3
SEP	0.728	0.839	0.912	0.731	0.754
r^2_{ncv}	0.904	0.885	0.629	0.901	0.856
SEE	0.409	0.453	0.786	0.420	0.500
F value	144.227	86.194	81.224	101.824	91.212
P value	0.00	0.00	0.00	0.00	0.00
steric	52.9	100		53.0	54.1
electrostatic	47.1		100	43.8	44.8
ClogP/CMR				3.2	1.1
r^2_{pred}	0.746	0.730	0.470	0.704	0.711
r^2_{bs}[b]	0.917	0.905	0.645	0.922	0.867
standard deviation[b]	0.025	0.025	0.055	0.020	0.037

[a] S = steric. E = electrostatic. [b] Results of bootstrapping analysis (100 samplings).

In an attempt to improve the statistical results of the present CoMFA model, various analyses were performed in which different CoMFA/PLS analysis parameters were varied. The QSAR analysis using rule-based Gasteigier−Marsilli charges showed a reduced cross-validated r^2 of 0.393 (data not shown), suggesting the importance of semiempirical charges in the CoMFA study of mazindol analogues. The CoMFA fields were also calculated using a grid spacing of 1 Å. The PLS analysis with AM1 charges and 1 Å grid spacing showed a cross-validated r^2 of 0.630. In another set of analyses on fields calculated using a grid spacing of 2 Å, the σ value (column filter) was varied. This value determines the selection of descriptor column with significant variation among different inhibitors. The smaller σ values lead to inclusion of many energy descriptors in the PLS analysis. This may sometimes improve the statistical significance of the model (signal); however, if these additional descriptors do not contribute to the CoMFA model, then they will increase its complexity (noise). Therefore, a reasonable balance of predictivity and signal-to-noise ratio has to be derived. The default value of 2.0 kcal/mol gave the best performance of predictivity and signal-to-noise ratio.

To explore the inclusion of additional descriptors in CoMFA, we calculated different descriptors on these compounds. The results from inclusion of these descriptors are presented in Table 8. CoMFA studies were also performed when steric and electrostatic fields were calculated separately. As can be seen from Table 8, a reasonably correlative and predictive model could be obtained when only steric fields were considered. This shows that variation in observed biological activity can be explained from the steric interactions of the compounds. When only electrostatic fields were considered, the CoMFA models showed reduced internal consistency (r^2_{cv} = 0.501). The PLS analysis using both fields, however, gave a better correlation (Table 7) than when these fields were used separately. Therefore, both steric and electrostatic interactions are important to explain the variance in biological activity. The lipophilicity of the molecules was calculated by the ClogP module, and the PLS analysis with inclusion of ClogP showed a slightly improved cross-validated r^2 value. In this model ClogP contributions were up to 3.2%; however, when

this model was used to predict the activity of test set compounds, a slight reduction in r^2_{pred} (0.704) was observed. Therefore, lipophilicity of these molecules may not be a determining factor for activity on the DAT. A steric parameter "CMR", i.e., molar refractivity, was included with steric and electrostatic fields from the CoMFA study. Although the QSAR models were reasonably correlative and predictive, the contributions by CMR were only 1.1%. Therefore, molar refractivity does not contribute to the CoMFA model. Thus, the CoMFA results for alignment I obtained from default parameters were compared with the results from alternative alignments.

The CoMFA from alignment II in which a heteroatom was not chosen for superimposition showed a small decrease in cross-validated r^2 (0.667) with two components. The non-cross-validated (0.821) and predictive (0.657) r^2 values were also less than those from alignment I. The visual analysis of this alignment showed orientations similar to those of alignment I except for some open-chain compounds.

The alignment rule III in which one of the phenyl rings was not selected for superimposition showed a lower r^2_{cv} of 0.566 with a non-cross-validated r^2 of 0.810. This model had a poorer predictive ability (r^2_{pred} = 0.619). The graphical analysis of molecules using alignment III showed that open-chain compounds were not aligned optimally. This suggests that the superimposition of this ring (ring D) is important for binding with the DAT.

In alignment IV, where ring C was not used for superimposition, some improvement in the r^2_{cv} value was observed but it had less external predictivity. Similarly, when ring A (alignment V) was excluded, the correlative and predictive power of the CoMFA was significantly reduced, suggesting that ring A is also essential for activity. Since alignment I used the centroids of the rings, because of changes in the size of the ring A, the position of the centroid could vary. Thus, another alignment (alignment VI) was derived where the "N" atom of ring A was selected instead of the centroid. There was no improvement in the statistical significance with this model. Thus, the results from these CoMFA studies suggest that the relative orientation of the two aromatic rings (C and D) and the placement of the heteroatom are essential for binding with the DAT. Ring A can be involved in steric interactions along with electrostatic interactions due to the nitrogen atoms. Deletion of one of the superimposing elements leads to a decrease in the correlative and predictive properties of the CoMFA model. During these alignments, open-chain compounds were found to orient their binding groups away from those of the tricyclic structure. Only when all four centers were selected could these compounds be fitted onto the template. Open-chain compounds were conformationally more flexible because they contain many rotatable bonds. Thus, loss in activity of these compounds is due to conformational flexibility and nonsuperimposibility on the template structure in the lowest energy conformation. However, this does not mean that all conformationally restricted cyclic analogues will be more active, since the substitution pattern of the aromatic rings will also determine the affinity toward the DAT.

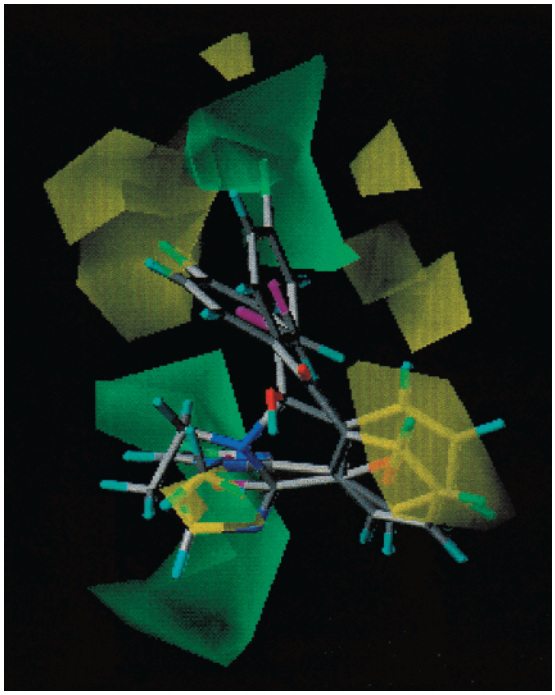

Figure 3. CoMFA steric STD DEV × COEFF contour plots with alignment I. Sterically favored areas are represented as green polyhedra. Sterically disfavored areas are represented by yellow polyhedra. The compounds **2** and **52** are shown.

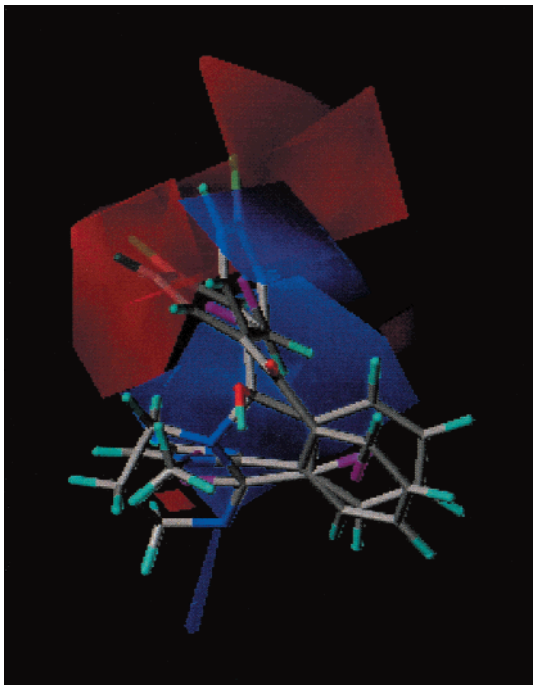

Figure 4. CoMFA electrostatic STD DEV × COEFF contour plots with alignment I. Positive charge-favored areas are represented by blue polyhedra. Negative charge-favored areas are represented by red polyhedra. The compounds **2** and **52** are shown.

The CoMFA steric and electrostatic contour maps are shown in Figures 3 and 4, respectively. The field values were calculated at each grid point as the scalar product of the associated QSAR coefficient and the standard deviation of all values in the corresponding column of the data table (STD DEV × COEFF) and are plotted as a percentage contributing to the QSAR equation. The green contours represent regions of high steric tolerance,

while yellow contours represent regions of unfavorable steric effects. The sterically favored green contours can be seen in Figure 3 around the heterocyclic ring (ring A) and ring D. The most active compound **2** shown in Figure 3 has a pyrimidine and phenyl ring within these favorable regions. Therefore, compounds with larger substitutions on these two rings are essential for high activity. A less active compound **52** is also shown in Figure 3, which has its ring D oriented in an unfavorable yellow contour. Also, the *N*-methyl group on ring A was found to overlap a small yellow contour, which will be detrimental to its activity. Compounds **40**−**42** show less activity because they have smaller substitutions in place of ring D, which will be ineffective to maintain necessary interactions in the sterically favored green region. These green fields around ring D are surrounded by sterically unfavored yellow contours. Compounds such as **18**, **19**, **T29**, and **T33** have reduced affinity, since the larger substituents on the phenyl ring orient into this unfavored yellow region. Adjacent placement of these yellow contours around the green regions suggests that not only substituents but also the orientation of this phenyl ring will be important for optimal binding. Compounds **6**−**8**, having ortho substituents on this phenyl ring (ring D), showed reduced activity compared to their meta- or para-substituted counterparts, since they will have different orientations of this ring. The presence of a green contour near the heterocyclic ring (ring A) suggests the presence of a large binding pocket in this region. Also, a sterically unfavored yellow field could be observed near ring C of these analogues, suggesting a restricted binding pocket in this region of the DAT. The steric contour suggests that ring C must be binding in a smaller pocket, whereas ring D must be orienting in a wider groove, which can tolerate larger substitution. However, very large substitutions on this ring will sterically overlap unfavorably on the adjacent yellow contour, thus reducing binding affinity.

The electrostatic contour plot is shown in Figure 4. The blue contours describe regions where positively charged groups enhance activity and red contours describe regions where a negatively charged group enhances activity. The electrostatic contour plots were localized around the phenyl ring (ring D). Therefore, not only is this ring important for steric interactions but the substituents on this ring will determine the electrostatic interactions of these compounds as well. The substitution of a halogen in the meta position of the phenyl ring (**11** and **39**) shows more activity than the para-substituted analogues (**13** and **1**). Therefore, the electron-withdrawing substituents at the meta position, located in the blue region, will be favorable, whereas electron-rich atoms in the para position, overlapping the red contours, are unfavorable for activity. Another large red contour was found surrounding the phenyl ring (ring D). This once again shows that the orientation of this ring will be important for binding with the DAT because a change in the orientation of the aromatic ring, due to ortho substitution, leads to overlap in this negative-charge-favoring region.

Several studies using mutants and chimeras of monoamine transporters have shown the importance of hydrophobic interactions for binding with transporters.[35−37] Thus, the aromatic rings C and D of mazindol analogues may simultaneously be involved in hydrophobic interactions with transmembrane domains of the DAT. The favoring regions were found to be in proximity to the unfavored regions, suggesting the importance of the conformational orientation of these rings. Removal or substitution with sterically bulky groups leads to complete loss of affinity due to loss in these interactions. The electrostatic interactions may assist in optimal binding with the transporter. The decrease in the statistical significance in the CoMFA model from alignment II where a heteroatom was not chosen suggests that the hydroxyl group is involved in hydrogen bonding or ionic interactions. The SAR of mazindol analogues and species scanning mutagenesis studies with monoamine transporters have also shown the importance of hydroxyl group interactions.[38]

The lack of studies on mutants of the DAT with mazindol or its analogues prevents direct extrapolation of the present observation to identify the binding site. However, the comparison of the contour maps derived from the CoMFA studies performed on other dopamine uptake inhibitors may provide some information about the ligand-binding characteristics of the DAT. A preliminary comparison of the CoMFA contour maps with structural features of the DAT ligands used to generate them was made to determine if there were any similarities.[32−34,39−41] All the contour analyses suggest that binding of these structurally diverse ligands is driven by the hydrophobic groups, which should be in optimum three-dimensional orientations. The differences in the patterns of CoMFA fields suggest that DAT can accommodate structurally diverse compounds having one or two hydrophobic rings with or without a basic nitrogen or its ring equivalents. Therefore, DAT must have a flexible binding region, and depending on the ligand bound, it adopts a suitable conformation by movement of transmembrane helices. It has been proposed that structurally distinct dopamine uptake inhibitors may access unique binding sites or may bind in different modes at the same or overlapping sites, thereby inducing a conformational change in the DAT that differentially effects dopamine uptake.[5,42−45] Further investigation of binding site topology using structurally divergent DAT ligands will provide tools with which to elucidate the structure and function of the DAT.

In summary a 3D-QSAR model using CoMFA was derived from a set of mazindol analogues binding to the DAT. A set of alignment rules was derived on the basis of the atom/centroids of the compounds. These alignment rules superimpose the molecules in different relative orientations, which will test the importance of different functional groups for binding to DAT. A highly correlative and predictive model was obtained. Inclusion of additional descriptors or use of steric and electrostatic fields separately did not improve the significance of the CoMFA models. Clearly, the steric and electrostatic fields of these compounds are adequate descriptors to explain the structure−activity relationships. The contour analysis showed the importance of the relative orientation of the two hydrophobic groups and the placement of a heteroatom of the mazindol analogues. The existence of favoring and unfavoring regions in proximity suggests that conformational orientation of the hydrophobic groups is important for activity. The

contour maps from this study will help in the design of new mazindol analogues and in the understanding of molecular interactions that are required for optimal DAT binding.

Acknowledgment. S.S.K. was supported by a National Institutes of Health Visiting Fellowship. This research was supported in part by the National Institute on Drug Abuse—Intramural Research Program. W.J.H. was supported by Grant R01 DA10533 from the National Institute on Drug Abuse (NIDA). We thank Theresa A. Kopajtic for the biological assays, Dr. Brian Hoffman for a critical reading of an earlier version of the manuscript, and Dr. Jamie Biswas of NIDA for coordination.

References

(1) Kuhar, M. J.; Ritz, M. C.; Boja, J. W. The Dopamine Hypothesis of the Reinforcing Properties of Cocaine. *Trends Neurosci.* **1991**, *14*, 299−301.

(2) Ritz, M. C.; Lamb, R. J.; Goldberg, S. R.; Kuhar, M. J. Cocaine Receptors on Dopamine Transporters Are Related to Self-Administration of Cocaine. *Science* **1987**, *237*, 1219−1223.

(3) Dewit, H.; Wise, R. A. Blockade of Cocaine Reinforcement in Rats with the Dopamine Receptor Blocker Pimozide But Not with the Noradrenergic Blockers Phentolamine and Phenoxybenzamine. *Can. J. Psychol.* **1977**, *31*, 195−203.

(4) Carroll, F. I.; Lewin, A. H.; Kuhar, M. J. In *Neurotransmitter Transporters: Structure, Function and Regulation*; Rieth, M. E. A., Ed.; Human Press, Inc.: Totowa, NJ, 1997; pp 263−295.

(5) Newman, A. H. Novel Dopamine Transporter Ligands: The State of the Art. *Med. Chem. Res.* **1998**, *8*, 1−11.

(6) Rothman, R. B.; Glowa, J. R. A Review of the Effects of Dopaminergic Agents on Humans, Animals, and Drug-Seeking Behavior, and Its Implications for Medication Development. *Mol. Neurobiol.* **1995**, *11*, 1−19.

(7) Carroll, F. I.; Howell, L. L.; Kuhar, M. J. Pharmacotherapies for Treatment of Cocaine Abuse: Preclinical Aspects. *J. Med. Chem.* **1999**, *42*, 2721−2736.

(8) Newman, A. H. Novel Pharmacotherapies for Cocaine Abuse 1997−2000. *Expert Opin. Ther. Pat.* **2000**, *10*, 1095−1122.

(9) Shimada, S.; Kitayama, S.; Lin, C. L.; Patel, A; Nanthakumar, E.; Gregor, P.; Kuhar, M.; Uhl, G. Cloning and Expression of a Cocaine-Sensitive Dopamine Transporter Complementary DNA. *Science* **1991**, *254*, 576−578.

(10) Kilty, J. E.; Lorang, D. B.; Amara, S. G. Cloning and Expression of a Cocaine-Sensitive Rat Dopamine Transporter. *Science* **1991**, *254*, 578−579.

(11) Usdin, T. B.; Mezey, E.; Chen, C.; Brownstein, M. J.; Hoffman, B. J. Cloning of the Cocaine-Sensitive Bovine Dopamine Transporter. *Proc. Natl. Acad. Sci. U.S.A.* **1991**, *88*, 11168−11171.

(12) Giros, B.; Mestikawy, S. E.; Godinot, N.; Zheng, K.; Han, H.; Yang-Feng, T.; Caron, M. G. Cloning, Pharmacological Characterization, and Chromosome Assignment of the Human Dopamine Transporter. *Mol. Pharmacol.* **1992**, *42*, 383−390.

(13) Javitch, J. A.; Blaustein, R. O.; Snyder, S H. [^{3}H] Mazindol Binding Associates with Neural Dopamine and Norepinephrine Uptake Sites. *Mol. Pharmacol.* **1984**, *26*, 35−44.

(14) Heikkila, R. E.; Cabbat, F. S.; Manzino, L.; Babington, R. G.; Houlihan, W. J. Unexpected Differences between Mazindol and Its Homologs on Biochemical and Behavioral Responses. *J. Pharmacol. Exp. Ther.* **1981**, *217*, 745−749.

(15) Heikkila, R. E.; Babington, R. G.; Houlihan, W. J. Pharmacological Studies with Several Analogues of Mazindol: Correlation between Effects on Dopamine Uptake and Various in Vivo Responses. *Eur. J. Pharmacol.* **1981**, *71*, 277−286.

(16) Kozikowski, A. P.; Liang, L.; Tanaka, J.; Bergman, J. S.; Johnson, K. M. Use of Nitrile Oxide Cycle Addition (NOC) Chemistry in the Synthesis of Cocaine Analogues; Mazindol Binding and Dopamine Uptake Studies. *Med. Chem. Res.* **1991**, *1*, 312−321.

(17) Johnson, K. M.; Bergman, J. S.; Kozikowski, A. P. Cocaine and Dopamine Differentially Protect [^{3}H] Mazindol Binding Sites from Alkylation by *N*-Ethylmaleamide. *Eur. J. Pharmacol.* **1992**, *227*, 411−415.

(18) Reith, M. E.; Selemeci, G.; Radiolabeling of Dopamine Uptake Sites in Mouse Striatum; Comparison of Binding Sites for Cocaine, Mazindol and GBR 12935. *Naunyn-Schmiedesberg's Arch. Pharmacol.* **1992**, *345*, 309−318.

(19) Izenwasser, S.; Terry, P.; Heller, B.; Witkin, J. M.; Katz, J. L. Differential Relationships among Dopamine Transporter Affinities and Stimulant Potencies of Various Uptake Inhibitors. *Eur. J. Pharmacol.* **1994**, *263*, 277−283.

(20) Chait, L. D.; Uhlenhuth, E. H.; Johanson, C. E. Reinforcing and Subjective Effects of Several Anorectics in Normal Human Volunteers. *J. Pharmacol. Exp. Ther.* **1987**, *242*, 777−783.

(21) Chait, L. D.; Uhlenhuth, E. H.; Johanson, C. E. The Discriminative Stimulus and Subjective Effects of Phenylpropanolamine, Mazindol and D-Amphetamine in Humans. *Pharmacol. Biochem. Behav.* **1986**, *24*, 1665−1672.

(22) Gotestam, K. G. Investigations of Abuse Potential of Anorectic Drugs. *Curr. Med. Res. Opin.* **1979**, *6*, 125−134.

(23) Margolin, A.; Avants, S. K.; Kosten, T. R. Mazindol for Relapse Prevention to Cocaine Abuse in Methadone-Maintained Patients. *Am. J. Drug Alcohol Abuse* **1995**, *21*, 469−481.

(24) Houlihan, W. J.; Boja, J. W.; Parrino, V. A.; Kopajtic, T. A.; Kuhar, M. J. Halogenated Mazindol Analogues as Potential Inhibitors of the Cocaine Binding Site at the Dopamine Transporter. *J. Med. Chem.* **1996**, *39*, 4935−4941.

(25) Houlihan, W. J.; Kelly, L.; Pankuch, J.; Koletar, J.; Kopajtic, T. A. Mazindol Analogues as Potential Inhibitors of the Cocaine Binding Site at the Dopamine Transporter. *J. Med. Chem.* **2002**, *45*, 4097−4109.

(26) Houlihan, W. J.; Ahmad, U. F.; Koletar, J.; Brand, L.; Kopajtic, T. A. Benzo- and Cyclohexanomazindols as Potential Inhibitors of the Cocaine Binding Site at the Dopamine Transporter. *J. Med. Chem.* **2002**, *45*, 4110−4118.

(27) Houlihan, W. J.; Boja, J. W.; Kopajtic, T. A.; Kuhar, M. J.; Degrado, S. J.; Toledo, L. Positional Isomers and Analogs of Mazindol as Potential Inhibitors of the Cocaine Binding Site on the Dopamine Transporter Site. *Med. Chem. Res.* **1998**, *8*, 77−90.

(28) Cramer, R. D., III.; Patterson, D. E.; Bunce, J. D. Comparative Molecular Field Analysis (CoMFA). 1. Effect of Shape on Binding of Steroids to Carrier Proteins. *J. Am. Chem. Soc.* **1988**, *110*, 5959−5967.

(29) Dewar, M. J. S.; Zoebisch, E. G.; Healy, E. F.: Stewart, J. J. P. AM1: A New General Purpose Quantum Mechanical Molecular Model. *J. Am. Chem. Soc.* **1985**, *107*, 3902−3909.

(30) Rodier, N.; Agafonov, V.; Cense, J. M.; Galinier, E.; Ombetta, J. E.; Frangin, Y.; Guilloteau, D. 5-(3-Iodophenyl)-2,3-dihydro-5-hydroxy-5*H*-imidazo[2,1-a]isoindole. *Acta Crystallogr.* **1993**, *C49*, 841−843.

(31) Aeberli, P.; Eden, P.; Gogerty, J. H.; Houlihan, W. J.; Penberthy, C. 5-Aryl-2,3-dihydro-5*H*-imidazo[2,1-*a*]isoindol-5-ols. A Novel Class of Anorectic Agents. *J. Med. Chem.* **1975**, *18*, 177−182.

(32) Carroll, F. I.; Mascarella, S. W.; Kuzemko, M. A.; Gao, Y.; Abraham, P.; Lewin, A. H.; Boja, J. W.; Kuhar, M. J. Synthesis, Ligand Binding, and QSAR (CoMFA and Classical) Study of 3β-(3′-Substituted phenyl)-, 3β-(4′-Substituted phenyl)-, and 3β-(3′,4′-Disubstituted phenyl)tropane-2β-carboxylic Acid Methyl Esters. *J. Med. Chem.* **1994**, *37*, 2865−2873.

(33) Lieske, S. F.; Yang, B.; Eldefrawi, M. E.; MacKerell, A. D., Jr.; Wright, J. (−)-3β-Substituted Ecgonine Methyl Esters as Inhibitors for Cocaine Binding and Dopamine Uptake. *J. Med. Chem.* **1998**, *41*, 864−876.

(34) Robarge, M. J.; Agoston, G. E.; Izenwasser, S.; Kopajtic, T.; George, C.; Katz, J. L.; Newman, A. H. Highly Selective N-Substituted 3α-[Bis(4′-fluorophenyl)methoxy]tropane Analogues for the Dopamine Transporter: Synthesis and Comparative Molecular Field Analysis. *J. Med. Chem.* **2000**, *43*, 1085−1093.

(35) Chen, N.; Reith, M. E. A. Structure and Function of the Dopamine Transporter. *Eur. J. Pharmacol.* **2000**, *405*, 329−339.

(36) Lin, Z.; Wang, W.; Uhl, G. R. Dopamine Transporter Tryptophan Mutants Highlight Candidate Dopamine- and Cocaine-Selective Domains. *Mol. Pharmacol.* **2000**, *58*, 1581−1592.

(37) Lin, Z.; Wang, W.; Kopajtic, T.; Revay, R. S.; Uhl, G. R. Dopamine Transporter: Transmembrane Phenylalanine Mutations Can Selectively Influence Dopamine Uptake and Cocaine Analog Recognition. *Mol. Pharmacol.* **1999**, *56*, 434−447.

(38) Barker, E. L.; Perlman, M. A.; Adkins, E. M.; Houlihan, W. J.; Pristupa, Z. B.; Niznik, H. B.; Blakely, R. D. High Affinity Recognition of Serotonin Transporter Antagonists Defined by Species-Scanning Mutagenesis. *J. Biol. Chem.* **1998**, *273*, 19459−19468.

(39) Carroll, F. I.; Gao, Y.; Rahman, M. A.; Abraham, P.; Parham, P.; Lewin, A. H.; Boja, J. W.; Kuhar, M. J. Synthesis, Ligand Binding, QSAR, and CoMFA Study of 3β-(*p*-Substituted phenyl)-tropane-2β-carboxylic Acid Methyl Esters. *J. Med. Chem.* **1991**, *34*, 2719−2725.

(40) Kotian, P.; Mascarella, S. W.; Abraham, P.; Lewin, A. H.; Boja, J. W.; Kuhar, M. J.; Carroll, F. I. Synthesis, Ligand Binding, and Quantitative Structure−Activity Relationship Study of 3β-(4′-Substituted phenyl)-β-heterocyclic Tropanes: Evidence for an Electrostatic Interaction at the 2β-Position. *J. Med. Chem.* **1996**, *39*, 2753−2763.

(41) Newman, A. H.; Izenwasser, S.; Robarge, M. J.; Kline, R. H. CoMFA Study of Novel Phenyl Ring-Substituted 3α-(Diphenylmethoxy)tropane Analogues at the Dopamine Transporter. *J. Med. Chem.* **1999**, *42*, 3502−3509.
(42) Vaughan, R. A.; Agoston, G. A.; Lever, J. R.; Newman, A. H. Differential Binding of Tropane-Based Photoaffinity Ligands on the Dopamine Transporter. *J. Neurosci.* **1999**, *19*, 630−636.
(43) Vaughan, R. A.; Gaffaney, J. D.; Lever, J. R.; Reith, M. A.; Dutta, A. K. Dual Incorporation of Photoaffinity Ligands on Dopamine Transporters Implicates Proximity of Labeled Domains. *Mol. Pharmacol.* **2001**, *59*, 1157−1164.
(44) Meltzer, P. C.; Liang, A. Y.; Blundell, P.; Gonzalez, M. D.; Chen, Z.; George, C.; Madras, B. K. 2-Carbomethoxy-3-aryl-8-oxabicyclo-[3.2.1]octanes: Potent Non-Nitrogen Inhibitors of Monoamine Transporters. *J. Med. Chem.* **1997**, *40*, 2661−2673.
(45) Reith, M. E. A.; Berfield, J. L.; Wang, L. C.; Ferrer, J. V.; Javitch, J. A. The Uptake Inhibitors Cocaine and Benztropine Differentially Alter the Conformation of the Human Dopamine Transporter. *J. Biol. Chem.* **2001**, *276*, 29012−29018.

JM0102093